doi:10.1088/1742-6596/32/1/071 Sixth Edoardo Amaldi Conference on Gravitational Waves

Development of a control scheme of homodyne detection for extracting ponderomotive squeezing from a Michelson interferometer

Shihori Sakata[1], Seiji Kawamura[2], Shuichi Sato[2], Kentaro Somiya[3], Koji Arai[2], Mitsuhiro Fukushima[2], and Akio Sugamoto[1]

[1] Graduate School of Humanities and Sciences, Ochanomizu University, 2-1-1 Otsuka, Bunkyo-ku, Tokyo, 112-8610, Japan

[2] National Astronomical Observatory of Japan, 2-21-1 Osawa, Mitaka, Tokyo 181-8588, Japan

[3] Max-Planck-Institut für Gravitationsphysik, Am Mühlenberg 1, 14476 Golm, Germany

E-mail: `shihori.sakata@nao.ac.jp`

Abstract. We developed a control scheme of homodyne detection. To operate the homodyne detector as easy as possible, a simple Michelson interferometer is used. Here a motivation that the control scheme of the homodyne detection is developed is for our future experiment of extracting the ponderomotively squeezed vacuum fluctuations. To obtain the best signal-to-noise ratio using the homodyne detection, the homodyne phase should be optimized. The optimization of the homodyne phase is performed by changing a phase of a local oscillator for the homodyne detection from a point at which a signal is maximized. In fact, in this experiment, using the developed control scheme, we locked the Michelson interferometer with the homodyne detector and changed the phase of the local oscillator for the homodyne detection. Then, we measured signals quantity changed by changing the phase of the local oscillator for the homodyne detection. Here we used the output from the homodyne detection as the signal.

1. Introduction

Quantum noise is one of the noises in gravitational wave detectors. The quantum noise consists of shot noise and radiation pressure noise. A point at which the radiation pressure noise equals the shot noise is called the standard quantum limit (SQL) [1]. In the next-generation detectors, the sensitivity of the detector will be limited by the quantum noise at most of the frequencies. When the quantum noise can be regarded as vacuum fluctuations entering an interferometer from its anti-symmetric port [2, 3], the vacuum fluctuations will be ponderomotively squeezed [4] by back action force of mirror motion due to the fluctuating radiation pressure on test masses. The radiation pressure is attributed to the vacuum fluctuations. In case of detecting the ponderomotively-squeezed vacuum fluctuations along with the gravitational waves using a conventional readout scheme, with which the signal is maximized, the sensitivity is limited by the SQL. However, by using homodyne detection that is one of the quantum nondemolition devices [5], with which the SQL can be overcome, the sensitivity will be able to beat the SQL, since an optimization of the homodyne phase makes it the best signal-to-noise ratio.

There, in this experiment, we developed a control scheme of the homodyne detection. To operate the homodyne detector as easy as possible, a simple Michelson interferometer is used. Here a part of the operation of the homodyne detector would be basically the same as the Michelson interferometer with the homodyne detector, even if an interferometer such as Fabry-Perot Michelson interferometer were used to extract the ponderomotive squeezing in the future experiment. To obtain the best signal-to-noise ratio using the homodyne detection, the homodyne phase should be optimized. The optimization of the homodyne phase is performed by changing a phase of a local oscillator for the homodyne detection from a point at which a signal is maximized. In fact, in the experiment, using the developed control scheme, we locked the Michelson interferometer with the homodyne detector and changed the phase of the local oscillator for the homodyne detection. Then, we measured signals quantity changed by changing the phase of the local oscillator for the homodyne detection. Here we used the output from the homodyne detection as the signal.

2. Extraction of ponderomotively-squeezed vacuum fluctuations using a Michelson interferometer

In the experiment, to confirm the operation of the homodyne detection as easy as possible, the simple Michelson interferometer is used. A motivation that the control scheme of the homodyne detection is developed is for our future experiment of extracting the ponderomotively squeezed vacuum fluctuations. There, in this section, we verify whether the sensitivity can experimentally circumvent the SQL utilizing the ponderomotive squeezing in case of using the simple Michelson interferometer.

2.1. Input-output relations for a Michelson interferometer

We derive input-output relations for vacuum fluctuations entering and leaving the anti-symmetric port of the Michelson interferometer, referred to the journal [6], with arm lengths $\ell \sim 10\,\mathrm{cm}$, a beam splitter mass $M \sim 1\,\mathrm{kg}$, and end mirror masses m. The fields of the vacuum fluctuations entering the anti-symmetric port are expressed by two quadrature amplitudes $a_1(\Omega)$ and $a_2(\Omega)$ which are made by the combination of annihilation operators $a_\pm(\omega_0 \pm \Omega)$ [7, 8], as shown in Figure 1. Modulation at a frequency $\Omega = 2\pi \times 1\,\mathrm{kHz}$ of carrier light is attributed to mirror motion produced by radiation pressure due to the vacuum fluctuations and the gravitational waves. Laser light with power $I_0 \sim 1\,\mathrm{W}$ and an angular frequency $\omega_0 \sim 1.8\times10^{15}\,\mathrm{Hz}$ of a perfectly coherent state is injected from the symmetric port of the Michelson interferometer. Here the interferometer's noise assumes to be only the quantum noise. The gravitational waves with the amplitude h are regarded as coming into the interferometer. Since in this calculation all the losses are neglected, the reflectivity of the end mirror $\mathrm{r_E}$ is 1.

The vacuum fluctuations that leave the anti-symmetric port are expressed by quadrature amplitudes b_1 and b_2. The quadrature amplitudes $b_{1,2}$ are obtained by

$$b_1 = a_1\, e^{2i\Omega\ell/c}, \tag{1}$$

$$b_2 = (a_2 - \mathcal{K}_{\mathrm{MI}}\, a_1)\, e^{2i\Omega\ell/c} + \sqrt{2\mathcal{K}_{\mathrm{MI}}}\, \frac{h}{h_{\mathrm{SQL}}}\, e^{i\Omega\ell/c}, \tag{2}$$

where

$$h_{\mathrm{SQL}} = \sqrt{\frac{4\hbar}{m_r \Omega^2 \ell^2}} \tag{3}$$

is square root of noise spectral density h_{SQL} for the gravitational-wave signal at the SQL, and

$$\mathcal{K}_{\mathrm{MI}} = \frac{4 I_0 \omega_0}{m_r c^2 \Omega^2}, \qquad m_r = \frac{Mm}{M+m}, \tag{4}$$

are a coupling constant that converts the input a_1 into the output b_2, because of the mirror motion, and reduced mass m_r.

2.2. *Possibility of extraction of ponderomotively-squeezed vacuum fluctuations using a simple Michelson interferometer*

From the quadrature amplitudes $b_{1,2}$, a noise spectral density of the Michelson interferometer, in case of using the conventional readout scheme, is obtained by

$$S_h = \frac{h_{\mathrm{SQL}}^2}{2}\left(\frac{1}{\mathcal{K}_{\mathrm{MI}}} + \mathcal{K}_{\mathrm{MI}}\right). \tag{5}$$

The noise spectral density achieves the SQL, where the coupling constant $\mathcal{K}_{\mathrm{MI}} = 1$.

In case of using the homodyne detection, the noise spectral density is obtained by

$$S_h = \frac{h_{\mathrm{SQL}}^2}{2\mathcal{K}_{\mathrm{MI}}}\left(1 + (\cot\eta - \mathcal{K}_{\mathrm{MI}})^2\right), \tag{6}$$

where η is homodyne phase. When the homodyne phase is optimized to $\eta = \mathrm{arccot}\mathcal{K}_{\mathrm{MI}}$, the sensitivity can obtain the best signal-to-noise ratio. Here the homodyne phase η is adjusted to the frequency at the SQL. Then the sensitivity of the Michelson interferometer will be able to beat the SQL. On this condition, we calculate how much mass of the end mirror is needed to beat the SQL. The frequency at the SQL is set to $\Omega_{\mathrm{SQL}} = 2\pi \times 1\,\mathrm{kHz}$. From the result of the calculation, it is found we need the end mirror masses $m \sim 1\,\mathrm{ng}$. Since use of the masses $m \sim 1\,\mathrm{ng}$ in the experiment is not realistic, we need to use an interferometer other than the Michelson interferometer. Now we start to calculate experimental parameters to beat the SQL using Fabry-Perot Michelson interferometer. From the result of the calculation, the realistic parameter can be obtained. In the proceeding, the calculation is not described.

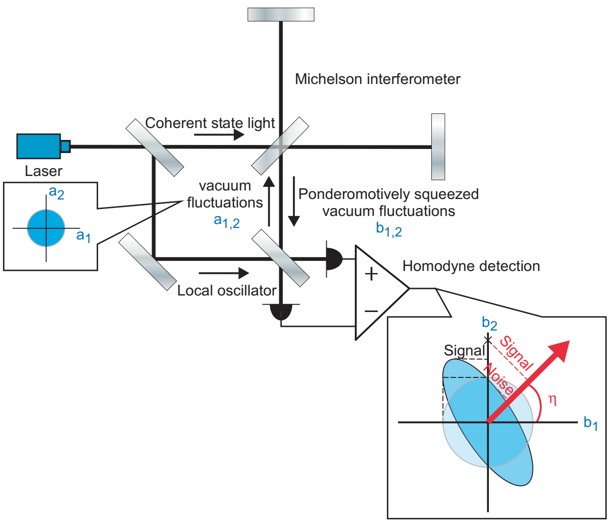

Figure 1. Schematic of homodyne detection introduced into a Michelson interferometer. Vacuum fluctuation that enters the anti-symmetric port of the Michelson interferometer is drawn by quadrature amplitudes $a_{1,2}$. Output vacuum, ponderomotively squeezed by the interaction of the Michelson interferometer, is drawn by an ellipse with the quadrature amplitude $b_{1,2}$ along with a gravitational-wave signal. The signal-to-noise ratio is optimized when the relative phase between the local oscillator and the amplitude of the field from the interferometer is set to $\eta = \mathrm{arccot}\mathcal{K}_{\mathrm{MI}}$.

3. Development of a control scheme for homodyne detection using a Michelson interferometer

We see from equation (6) that the homodyne phase should be adjusted to $\eta = \mathrm{arccot}\mathcal{K}_{\mathrm{MI}}$ to make the sensitivity the best signal-to-noise ratio. To be locked at the point that the homodyne phase is optimized, the phase of the local oscillator is changed from the point that the signal is maximized, as shown in Figure 1. In the experiment, to confirm the operation of the homodyne detection as easy as possible, we used the Michelson interferometer. Even if in the future the interferometer such as the Fabry-Perot Michelson interferometer is used, we think the part of the control of the homodyne detector is basically the same as the control using the Michelson interferometer. In this section, we describe the developed control scheme for the Michelson interferometer with the homodyne detector.

3.1. Experimental setup

The experimental setup is shown in Figure 2. Laser light (Nd:YAG 1064nm) with power $I_0 \sim 200\,\mathrm{mW}$ and an angular frequency ω_0 is split at a 50:50 beam splitter, BS1 called in Figure 2. Reflected light is the local oscillator for the homodyne detection. Transmitted light is phase modulated at an angular frequency $\omega_\mathrm{m} \sim 2\pi \times 18.8\,\mathrm{MHz}$. The modulated laser electric field E_in is

$$\begin{aligned} E_\mathrm{in} &= E_0\, e^{i\,(\omega_0 t + m\cos\omega_m t)} \\ &\simeq E_0\, e^{i\omega_0 t}\left[J_0(m) + iJ_1(m)\, e^{i\omega_m t} + iJ_1(m)\, e^{-i\omega_m t}\right], \end{aligned} \tag{7}$$

where $E_0 e^{i\omega_0 t}$ is the laser electric field, m is the modulation depth, and J_n is the nth order Bessel function. In the calculation, the approximation, $J_n(m) \sim 1/n!\,(m/2)^2\,(m \ll 1)$, is used. The modulated beam is incident into the Michelson interferometer, and then recombines at a 50:50 beam splitter, BS3 called in Figure 2. The recombined light at the anti-symmetric port and the local oscillator are split at a 50:50 beam splitter, BS2 called in Figure 2. Using the transmitted and reflected light from the BS2 beam splitter, the homodyne detection is performed. The output signal from the homodyne detection is

$$V_\mathrm{HD} = \frac{1}{2}|E_\mathrm{out} + E_\mathrm{LO}|^2 + |E_\mathrm{out} - E_\mathrm{LO}|^2 = 2\mathrm{Re}\,[E^*_\mathrm{out}\, E_\mathrm{LO}]\,, \tag{8}$$

where E_out is the recombining electric field at the anti-symmetric port, and E_LO is the electric field of the local oscillator. Note that all of the optics in the experiment are fixed on the table.

3.2. Development of a control scheme

The Michelson interferometer introducing the homodyne detector has two longitudinal degrees of freedom to be controlled. One is the differential length change l_- in the arm of the Michelson interferometer, and the other is the differential length change L_- in an arm of Mach-Zehnder interferometer, where the differential length change is given by $L_- = (L_1 - l_+) - L_2$. The inline and perpendicular arm lengths are given by ℓ_i and ℓ_p, respectively. Common and differential mode changes of the arm lengths are given by $\ell_+ = \ell_p + \ell_i$ and $\ell_- = \ell_p - \ell_i$, respectively. As shown in Figure 2, the gravitational-wave signals from the homodyne signal output V_GW can be obtained. The homodyne signal output V_GW from equation (8) is obtained by

$$V_\mathrm{GW} = -|E_0|^2\, \sin\eta \sin\phi, \tag{9}$$

where the phase $\phi = \omega_0 l_-/c$ is the differential phase shift of the Michelson interferometer, and the phase $\eta = \omega_0 L_-/c$ is the differential phase shift of the Mach-Zehnder interferometer. We can also extract the demodulated signals $V_\mathrm{Qhd} = -m/2|E_0|^2 \sin\alpha \sin\eta \cos\phi$ of the quadrature phase and $V_\mathrm{Ihd} = -m/2|E_0|^2 \cos\alpha \cos\eta \sin\phi$ of the in-phase from the RF portion of the homodyne signal.

Here when the Michelson interferometer is operated on dark fringe at the anti-symmetric port, we verify whether the two longitudinal degrees of freedom can be controlled. Then the derivation of the output signal V_GW becomes $\partial V_\mathrm{GW}/\partial\phi \propto \sin\eta$. The demodulated signals V_Qhd of the quadrature phase and V_Ihd of the in-phase become $V_\mathrm{Qhd} \propto \sin\alpha \sin\eta$ and $V_\mathrm{Qhd} \propto 0$, respectively. To control the two longitudinal degrees of freedom, the phase η should be locked around $\eta \sim 0$. If so, the homodyne signal output V_GW almost cannot be obtained. There a DC offset to the differential signal of the Michelson interferometer is added, as shown in Figure 2. The Michelson interferometer is locked at an operating point that moves a little from dark fringe. Then the phase η can be locked around $\eta \sim \pi/2$ that the signals are maximized. Since the derivation of the homodyne signal output is $\partial V_{\rm GW}/\partial\phi \propto \cos(\phi_{\rm off})$, where the phase shift ϕ adding the DC offset is given by $\phi_{\rm off}$, the Michelson interferometer can be locked.

In the experiment, to control the differential length change of the Michelson interferometer, we extracted the demodulated signal $V_{\rm Qmi}$ of the quadrature phase from the symmetric port of the Michelson interferometer. The derivation $\partial V_{\rm Qmi}/\partial\phi_{\rm off}$ is obtained by

$$\frac{\partial V_{\rm Qmi}}{\partial\phi_{\rm off}} = -\frac{m}{2}|E_0|^2 \sin\alpha\cos\beta, \tag{10}$$

where α and β are given by $\omega_m \ell_-/c$ and $\omega_m \ell_+/c$, respectively. In order to obtain the maximum signals, the local oscillator phase of the Michelson interferometer is adjusted to make the phase shift β zero. Here from equation (9) it is found that the differential length change of the Michelson interferometer can be also extracted from the homodyne signal output $V_{\rm GW}$. When the experiment to beat the SQL utilizing the ponderomotive squeezing is started, the extraction from the homodyne signal output $V_{\rm GW}$ would be better than the extraction from the symmetric port of the Michelson interferometer. To control the length change of the Mach-Zehnder interferometer, we extracted the demodulation signal $V_{\rm Imz}$ of the in-phase from the RF portion of the homodyne signal, as shown in Figure 2. The derivation $\partial V_{\rm Imz}/\partial\eta$ is

$$\frac{\partial V_{\rm Imz}}{\partial\eta} = -\frac{m}{2}|E_0|^2 \cos\alpha\sin(\phi_{\rm off}). \tag{11}$$

From the result of the calculation mentioned above, the Michelson interferometer was locked using the control signal from equation (10), and the Mach-Zehnder interferometer was locked using the control signal from equation (11). Also, the ponderomotively-squeezed vacuum fluctuations along with the gravitational-wave signals can be detected from the homodyne output signal $V_{\rm GW}$ of equation (9).

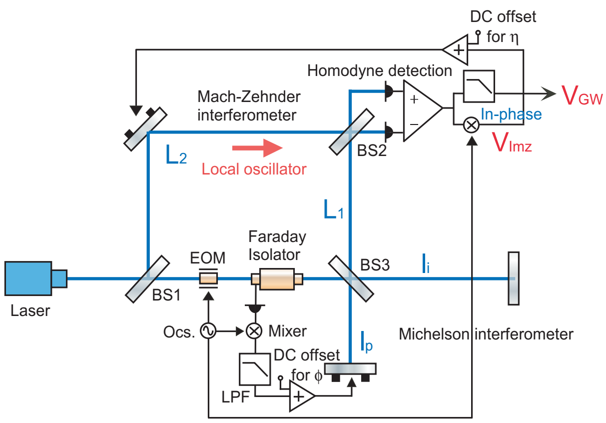

Figure 2. Schematic of the experimental setup. We call each of the 50:50 beam splitters BS1, BS2, and BS3. For the Michelson interferometer, the inline and perpendicular arm lengths are given by ℓ_i and ℓ_p, respectively. Common and differential mode changes of the arm lengths are given by $\ell_+ = \ell_p + \ell_i$ and $\ell_- = \ell_p - \ell_i$, respectively. For the Mach-Zehnder interferometer, the laser path lengths of the transmitted and reflected light divided by BS1 are given by L_1 and L_2, respectively.

4. Experimental results

Using the control scheme described in Section 3, we locked the Michelson interferometer with the homodyne detector at the point that the maximum homodyne signal output is obtained. To obtain the best signal-to-noise ratio using the homodyne detection, the homodyne phase should be optimized. The optimization of the homodyne phase is performed by changing a phase of a local oscillator for the homodyne detection from a point at which a signal is maximized. The phase of the local oscillator for the homodyne detection was changed by a DC offset added to the demodulation signal of the in-phase.

In the experiment, first when the DC offset was not added, we confirmed the maximum homodyne signal was obtained. Next, by adding the DC offset to the demodulation signal of the in-phase continuously, in proportional to $\sin\eta$ from equation (9), we confirmed the homodyne signal output quantity was changed continuously. In Figure 3, the homodyne signal output quantities, when the Michelson interferometer with the homodyne detector was locked at arbitrary homodyne phases, are shown.

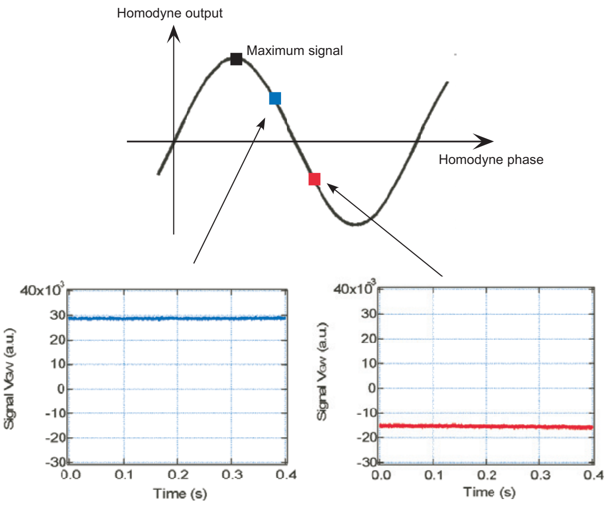

Figure 3. By adding the DC offset to the demodulation signal of the in-phase continuously, in proportional to $\sin\eta$ from equation (9), we confirmed the homodyne signal output quantity was changed continuously. In this Schematic, the homodyne signal output quantities, when the Michelson interferometer with the homodyne detector was locked at arbitrary homodyne phases, are shown.

5. Summary and future plan

Using the control scheme described in Section 3, we locked the Michelson interferometer with the homodyne detector at the point that the maximum homodyne signal output is obtained. We think a part of the operation of the homodyne detector would be basically the same as the Michelson interferometer with the homodyne detector, even if an interferometer such as Fabry-Perot Michelson interferometer were used to extract the ponderomotive squeezing in the future experiment.

By the way, in case of using the Michelson interferometer to beat the SQL utilizing the ponderomotively-squeezed vacuum fluctuations, as described in Section 2, we need the end mirror masses $m = 1\,\mathrm{ng}$ on the conditions of the laser power $I_0 \sim 1\,\mathrm{W}$ and the frequency $\Omega_{\mathrm{SQL}} = 2\pi \times 1\,\mathrm{kHz}$ at the SQL. The parameters are severe. In the future, we will start the experiment using the Fabry-Perot Michelson interferometer. From the result of calculating the experimental parameters, it is found that the parameters are realistic. Here the calculation is not described.

References

[1] Braginsky B V and Khalili Ya F 1996 *Rev. Mod. Phys.* **68** 1
[2] Caves M C 1980 *Phys. Rev. Lett.* **45** 75
[3] Caves M C 1981 *Phys. Rev.* D **23** 1693
[4] Braginsky B V and Manukin B A 1967 *Sov. Phys. JETP* **25** 653
[5] Braginsky B V 1968 *Sov. Phys. JETP* **26** 831
[6] Kimble J H, Levin Y, Matsko B A, Thorne S K, and Vyatchanin P S 2002 *Phys. Rev.* D **65** 022002
[7] Caves M C and Schumaker L B 1985 *Phys. Rev.* A **31** 3068
[8] Schumaker L B and Caves M C 1985 *Phys. Rev.* A **31** 3093